

TECHNICAL RESEARCH CENTRE OF FINLAND

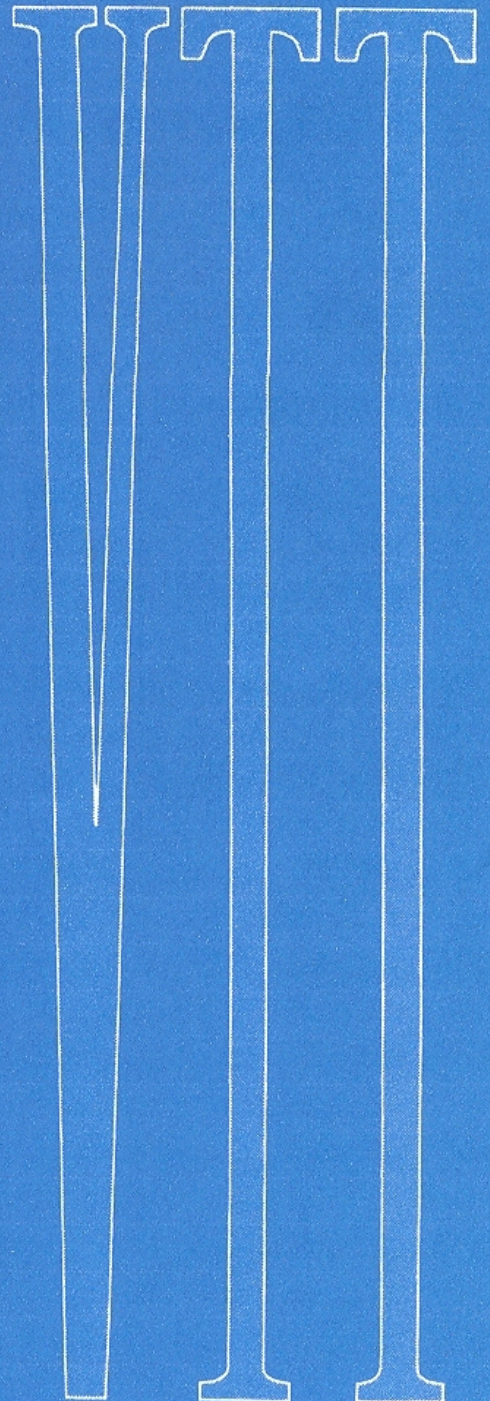
Electrical and  
Nuclear Technology

16

Matti Ojala  
Eero Leinonen

POSSIBLE METHODS FOR  
THE MEASUREMENT OF  
TRANSIENT INTER-  
MODULATION DISTORTION

VALTION TEKNILLINEN TUTKIMUSKESKUS  
Espoo 1975



TECHNICAL RESEARCH CENTRE OF FINLAND  
ELECTRICAL AND NUCLEAR TECHNOLOGY  
PUBLICATION 16

UDC 621.391.83:621.375

**POSSIBLE METHODS FOR THE MEASUREMENT OF TRANSIENT  
INTERMODULATION DISTORTION**

**MATTI OTALA and EERO LEINONEN**  
Electronics Laboratory

## Contents

	Page
Abstract . . . . .	5
1. Introduction . . . . .	5
2. Overshoot clipping method . . . . .	6
3. Square wave intermodulation method . . . . .	7
3.1 Sine wave - square wave measurement signal . . . . .	9
4. The pseudo-random noise method . . . . .	13
5. Conclusions . . . . .	15
References . . . . .	16

## Abstract

*Conventional distortion measurements do not always correlate with the audible quality of audio amplifiers. One possible reason for this is the transient intermodulation distortion, which is unpleasantly audible but lacks a commonly known easily performable measurement method.*

*Three new measurement methods are presented. They are the overshoot clipping method, the square-wave intermodulation method and the pseudo-random noise intermodulation method. The relative merits and drawbacks of the methods are discussed.*

## Introduction

Transient intermodulation distortion (TIM) arises when a forward path within a feedback loop is too slow to make the feedback circuit follow an input signal under transient condition (1) (2). The steep slope of a transient passes to input stages without the controlling characteristics of feedback, and therefore transient amplitude may excure beyond the linear region of the amplifier.

During the overload condition other simultaneous signals are distorted, the degree depending on the length and strength of the overload. In very heavy overload a proportion of simultaneous other signals may simply vanish.

It has been said that TIM is just another definition of slew rate and its existence can be deduced reliably by measuring the slew rate or power bandwidth. This is true in the case where the amplifier open-loop gain is linear until the abrupt overload level is reached. If, however, the open-loop transfer function has a »soft» s-form, the amplifier will already be excessively non-linear before the final overload level is reached. As seen from the output the amplifier remains linear due to feedback when measured with a »steady» sine wave test signal. Internally, however, the transients will intermodulate other simultaneous signals, which are amplified in transient condition by the non-linear part of the transfer function. The feedback will of course correct the non-linearity to a certain degree, but there will in any case be distortion, which is basically TIM although the slew rate is not exceeded.

The CCIF IM, or difference-frequency distortion measurement method seems to reveal TIM when two closely spaced high frequency test signals are used, but those two signals do not reveal very well the incremental gain decrease, which is a result of the TIM-overload.

Accordingly a more sensitive and more reliable method would be desirable.

Three possible methods are described in the present paper. The first one has already been outlined (2) and it is mainly an indicator of TIM. The second and third methods are capable of giving the amount of distortion as a percentage of the measurement signal.

### Overshoot clipping method

The power amplifier in Fig. 1 is driven by a low-pass filtered step  $V_2$  (Fig. 2). The frequency content of  $V_2$  lies within the closed-loop frequency response of the amplifier, but provided that the pole due to  $RC$  is lower in frequency than the upper cut-off frequency of the preamplifier, there exists a notable overshoot in the error voltage  $V_3$  (1), (2). The overshoot may overload stage  $A_1$  so that a momentary intermodulation burst arises.

In checking interloop transient behaviour of an amplifier the first step is to identify the slowest stage in the forward path. This is usually the point where the lag compensation of the amplifier is applied. Beyond this stage, the overshoot has been smoothed out. Before this stage the overshoot is present and may be suppressed if it exceeds the dynamic margins of the respective stages. The second step is to find the input signal level at which this suppression occurs. If this level is within the usual operating range, the amplifier will produce TIM under normal operation.

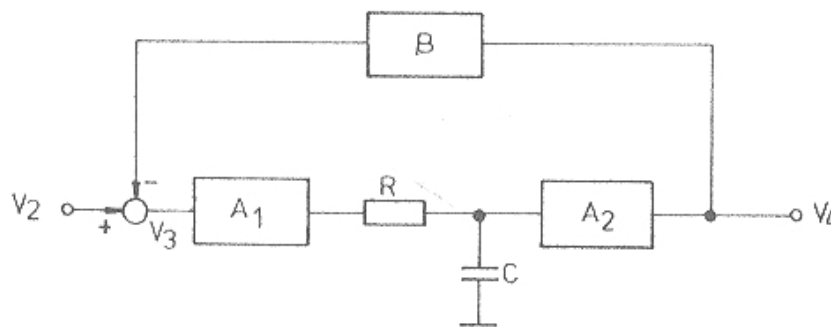


Fig. 1. A block diagram of a power amplifier.  $RC$  is the lag compensation and  $\beta$  is a purely resistive feedback loop.

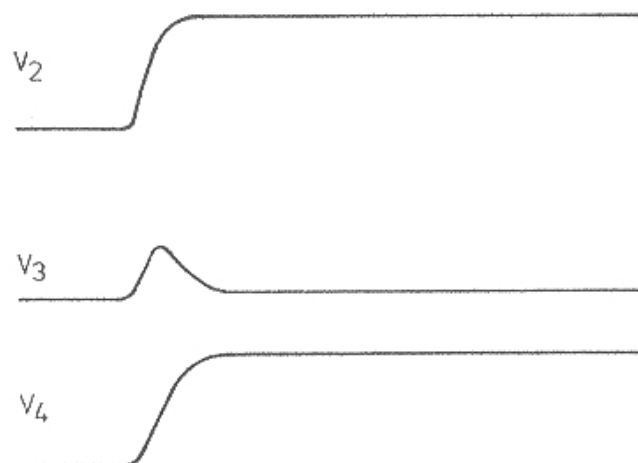


Fig. 2. Step response of the amplifier of Fig. 1.  $V_2$  and  $V_4$  are normal low pass filtered steps, but the error signal  $V_3$  has an overshoot due to  $RC$ .

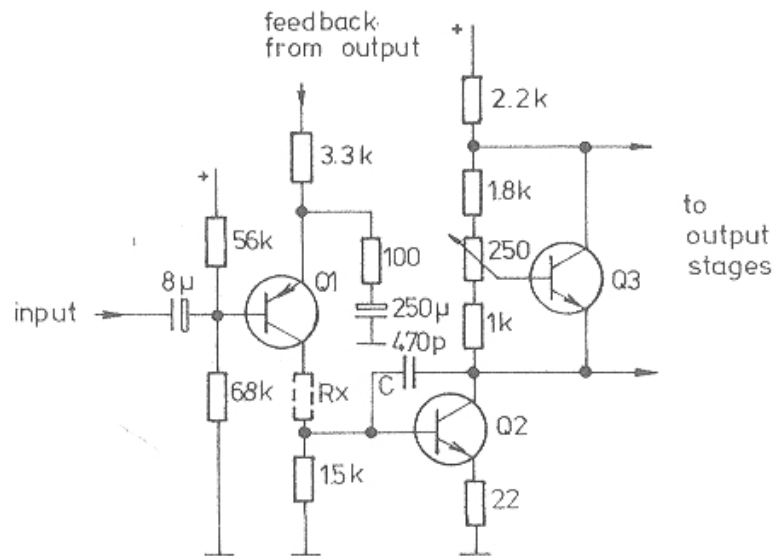


Fig. 3. The typical driver of a complementary symmetry power amplifier. The resistor  $R_x$  is inserted in the collector of  $Q_1$  for detection of current overshoot.

As an example consider the circuit of Fig. 3. It shows the typical driver stages of a complementary symmetry power amplifier. The slowness of the amplifier is concentrated in stage  $Q_2$  due to the compensating capacitor  $C$ . The overshoot to be studied appears at the collector of  $Q_1$  as this is the summing point of the input signal and the feedback signal. If  $V_3$  is overloaded, this will happen at the collector of  $Q_1$  because of the very low input impedance of the base of  $Q_2$  due to Miller effect. In this case the overload will be seen in the collector current of  $Q_1$ . This can be measured by inserting resistor  $R_x$  in series with the collector and by measuring the waveform across it.

By slowly increasing the input voltage and noting any changes in the ratio  $I_{peak}/I_{\infty}$ , the amount of TIM can be estimated from the level of which the overshoot suppression begins, and from the length of the overshoot but exact numbers cannot be given.

This measurement can be performed with standard equipment available in any laboratory, but as it requires penetration into the internal structure of the amplifier it is best suited to a designer. Although the method is not accurate it is very sensitive because it will even give information, when TIM is just about to appear.

### Square-wave intermodulation method

When the theory of TIM was published (1) (2), the open-loop gain was supposed to be linear until an abrupt overload level. In practice, however, the maximum output of  $A_1$  ( $V_{lim}$  in Fig. 4) may be preceded by large non-linearities far below it.

Let us consider a case, where the input signal consists of one step and other simultaneous signals. For convenience let the amplitude of those signals be so small compared with the non-linearity that the gain  $A_1$  may be regarded as piecewise linear for them.

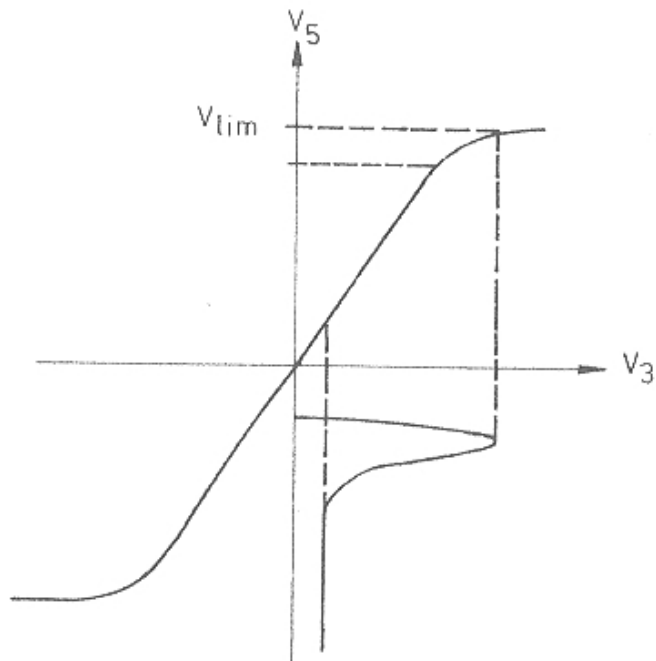


Fig. 4. Non-linear open-loop transfer function  $A'_1$  of the amplifier in Fig. 1.

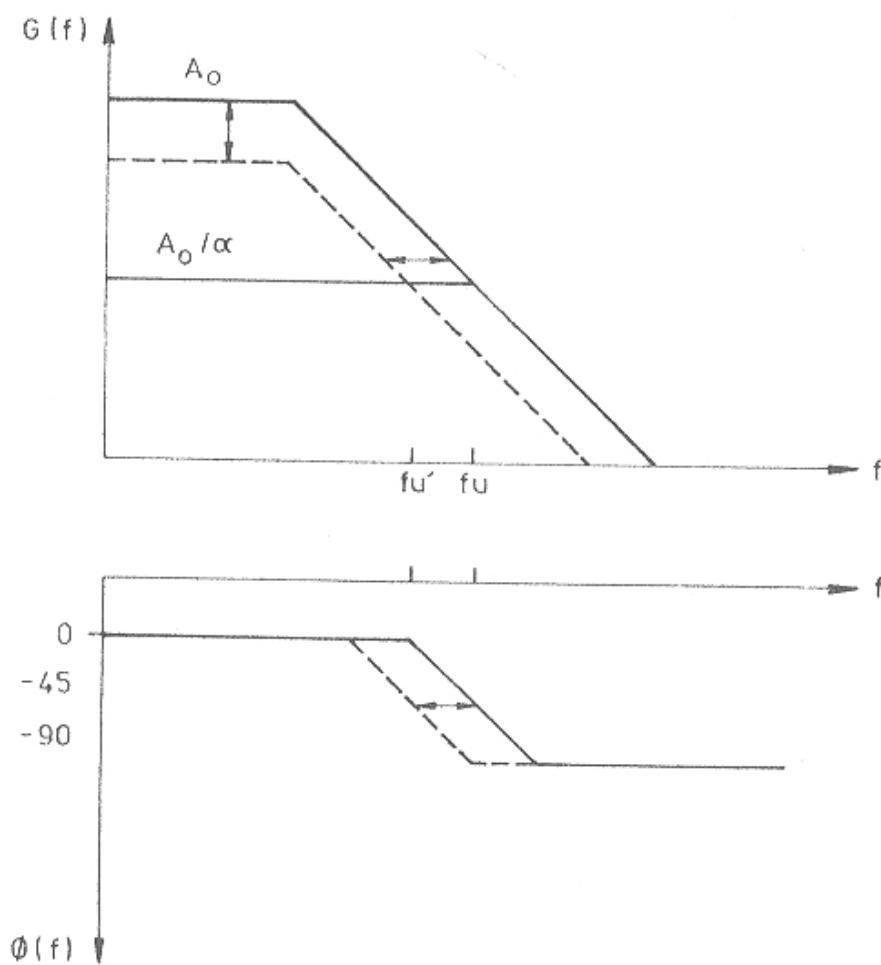


Fig. 5. Incremental gain decrease and phase change in the overload condition.

This gain may be called incremental gain and its value is the derivative of  $A_1$  (Fig. 4) at each operating point.

If a step causes a TIM-overload in  $A_1$ , the operating point for the other signals moves to the non-linear part of  $A_1$  and the open-loop incremental gain decreases. If the decrease is small compared with the feedback value, the closed-loop incremental gain does not change for low frequencies (Fig. 5). However, provided that the overload does not change the parameters of the frequency compensation, the closed-loop upper cut-off frequency decreases from  $f_u$  to  $f'_u$  (Fig. 5). The closed-loop incremental gain then decreases in the high frequency range between  $f'_u$  and  $f_u$  (Fig. 5), the decrease being in the upper cut-off frequency approximately equal to the decrease of the open-loop gain in  $A_1$ . In addition, a phase change is produced reaching even to frequencies as much as a decade below  $f'_u$  in Fig. 5. The most sensitive frequencies for the phase shift are those around a tenth of the upper cut-off frequency  $f_u$ , because in steady state condition they do not have notable phase shifts but at the moment that the incremental gain decreases, their phase will be changed. Accordingly, in overload condition the simultaneous signals will have a change in phase or both in phase and amplitude depending on the signal frequency and the degree of the overload. Fig. 6 shows incremental gain decrease and phase change with increasing overload degree to a signal, which is in frequency a tenth of the upper cut-off frequency, for an amplifier having an open-loop gain of 80 dB, a feedback of 60 dB and the exponential non-linear open-loop gain.

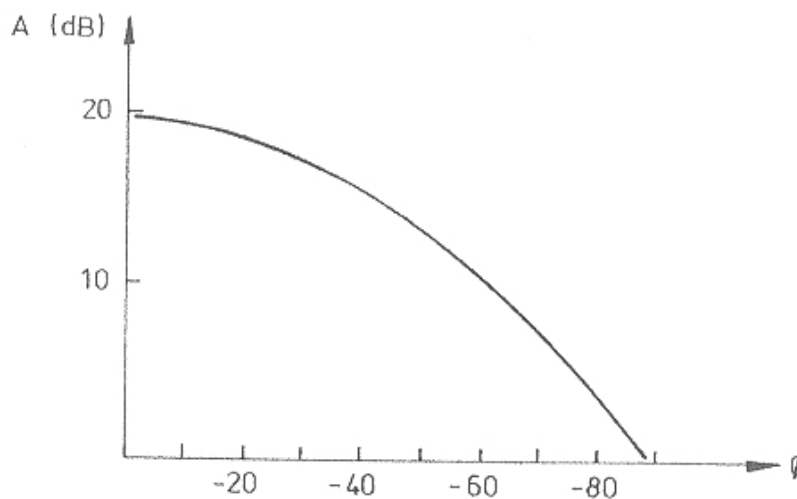


Fig. 6. Gain-phase shift curve with increasing overload degree to a signal, which has a frequency one decade below the upper cut-off frequency. The amplifier open-loop gain was 80 dB and feedback 60 dB.

#### Sine wave - square wave measurement signal

The test signal is a combination of a low-pass filtered square wave  $f_1$  and a sine wave  $f_2$ , which is higher in frequency and lower in amplitude as in Fig. 7a. If an amplifier produces TIM the square-wave transitions overload some of its stages, the gain for the sine wave decreases momentarily from  $A$  to  $A'$ , and the phase changes from  $\phi$  to  $\phi'$  (Fig. 7b). The sine wave is then both amplitude and phase modulated, depending on



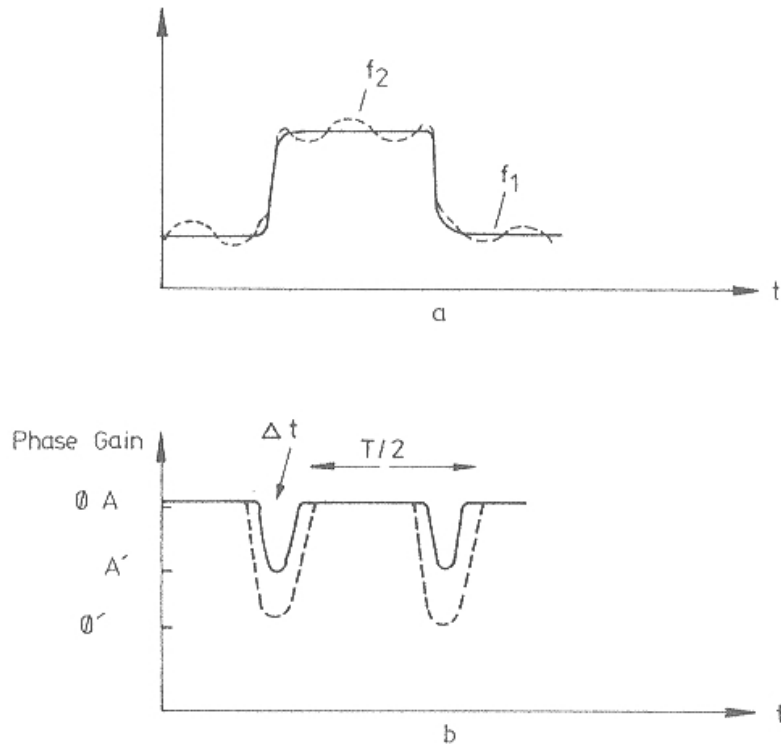


Fig. 7. Amplifier loading by sine wave - square wave signal. The gain for the sine wave decreases and the sine wave phase changes every time that the square wave overloads the amplifier.

the sine frequency  $f_2$  and on the degree of the overload. The modulating frequency is twice the square-wave frequency  $f_1$ , if the overload properties of the amplifier are such that both transitions of the square-wave period will cause an overload. If, however, the amplifier overloads only during one of the two transitions, the modulating frequency is  $f_1$ . The sine wave will have sidebands at frequencies  $f_2 \pm nf_1$ , where  $n$  is an integer depending on the overload characteristics of the amplifier. The resulting signal may be described as

$$f(t) = A(t)a_2 \sin(\omega_2 t + \phi(t)) \tag{1}$$

where

- $A(t)$  is the incremental gain
- $a_2$  is the amplitude of the sine wave
- $\omega_2$  is the angular frequency of the sine wave
- $\phi(t)$  is the phase of the sine wave
- $t$  is time

Equation (1) can be modified to

$$f(t) = A(t)a_2 [\sin \omega_2 t \cos \phi(t) + \cos \omega_2 t \sin \phi(t)] \tag{2}$$

To facilitate the analysis let us assume for a moment that  $\phi(t)$  is zero. The equation (2) then reduces to

$$f(t) = A(t)a_2 \sin \omega_2 t \quad (3)$$

In the frequency domain this appears as the spectrum of  $A(t)$ -envelope centered at angular frequency  $\omega_2$ .

Secondly, let us assume that the gain  $A(t)$  is constant  $A$ , and

$$\phi(t) = \begin{cases} -\rho & \text{during the overload } \Delta t (\rho < 90^\circ) \\ 0 & \text{otherwise} \end{cases}$$

Equation (2) then has the form

$$f(t) = Aa_2 [\sin \omega_2 t \cos \phi(t) + \cos \omega_2 t \sin \phi(t)] \quad (4)$$

The term  $\sin \omega_2 t \cos \phi(t)$  appears in the frequency domain exactly like equation (3). The term  $\cos \omega_2 t \sin \phi(t)$  can be calculated in the same way and the resulting frequency components overlap with the components of the first term, but the phase shift of 90 degrees must be taken into account before summation.

The frequency spectrum of the whole signal of the equation (2) can be calculated step by step first taking into account the components due to phase modulation and then calculating the effect of the amplitude modulation. These operations are time-consuming and because the frequency components from phase and amplitude modulation overlap, let us consider a simplified case, where the phase modulation is omitted.

The incremental gain envelope of Fig. 7b is assumed to have a form of pulse train with  $T/2 = 500 \mu\text{s}$  corresponding to a loading square-wave frequency of 1 kHz. The overload time  $\Delta t$  is assumed to be  $10 \mu\text{s}$ . Let us take a value of 20 dB for  $A$  and  $-\infty$  for

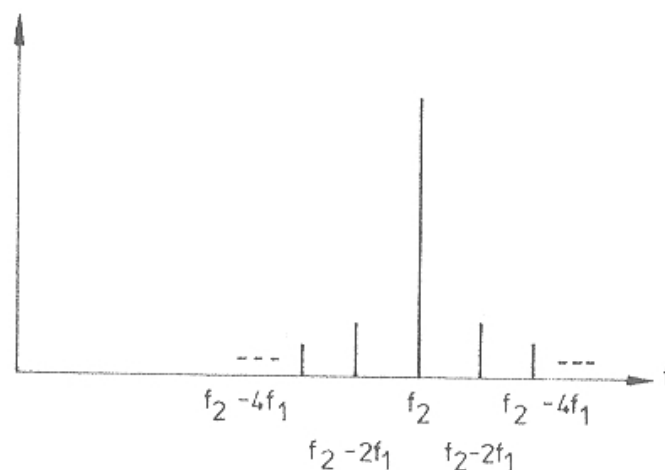


Fig. 8. Non-harmonic sidebands of the sine wave produced in sine wave - square wave loading.

$A'$ . If the attenuation of the lag compensation is not taken into account the sidebands will have the values of

	Frequency	Amplitude
Basic sine wave	$f_2$	$a_2$
Sidebands	$f_2 \pm 2f_1$	$\sim 2\%$ of $a_2$
	$f_2 \pm 4f_1$	$\sim 2\%$ of $a_2$
	$f_2 \pm 10f_1$	$\sim 2\%$ of $a_2$
	...	
	$f_2 \pm 20f_1$	$\sim 1,9\%$ of $a_2$

For an input signal spectrum as in Fig. 9a the resulting output spectrum may have the form shown in Fig. 9b.

If an amplifier produces TIM, a variety of sidebands will appear around the sine wave when the amplifier is loaded with a sine wave - square wave signal. The easiest way to detect the sidebands is to use a low frequency spectrum analyzer (4) and in this way the whole measurement can be performed without specially designed equipment the only problem being, of course, the poor resolution and low fundamental rejection of most spectrum analyzers. Another possibility is to pick up the sidebands with a high- $Q$  band-pass filter.

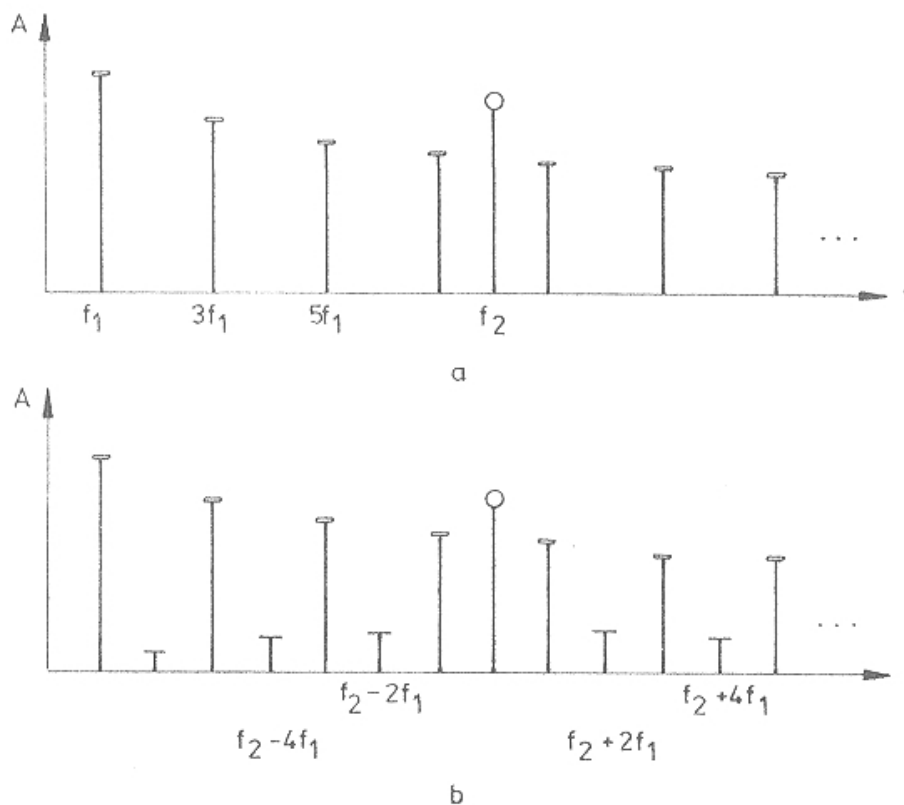


Fig. 9. (a) Frequency spectrum of the measurement signal, (b) Resulting output spectrum.

It makes sense to stabilize the spectrum of the measurement signal by locking  $f_1$  and  $f_2$  in frequency with each other. To make sure that the resulting sidebands do not overlap with the frequency components of the input signal,  $f_1$  and  $f_2$  should be selected so that

$$nf_1 < f_2 - mf_1 < (n+1)f_1 \quad (5)$$

where  $nf_1$  represents a harmonic component of the square wave and  $m$  represents the order of a sideband. Equation (5) can be modified by taking  $m+n=\nu$  to

$$\nu f_1 < f_2 < (\nu+1)f_1 \quad (6)$$

For an optimum result  $f_1$  and  $f_2$  should be selected so that

$$\frac{f_2}{f_1} = \sqrt{\nu(\nu+1)} \quad (7)$$

However, using frequencies selected by that criterion the sidebands of high order, which are mathematically negative in frequency would overlap with the sidebands of low order. The criterion of the optimum frequency relation  $f_2/f_1$  must therefore be modified to be

$$f_2/f_1 = \sqrt{(\nu+1)\sqrt{\nu(\nu+1)}} \quad (8)$$

Let us take a value for  $f_2$  of 15 kHz, which is the highest frequency which has standardized level limits in audio reproduction. Then only lower sidebands are interesting and final recommended values for  $f_1$  and  $f_2$  with  $\nu$  of 4, are 3,18 kHz and 15 kHz, respectively.

The level of TIM-sidebands depends on the selection of the measurement signal parameters. The overload time  $\Delta t$  (Fig. 7b) is constant for a given input signal. If the square-wave frequency increases the amplifier will stay in overload condition for proportionally longer time, and hence the amplitude of the sidebands will increase. Therefore details of parameters  $f_1, f_2$ , test signal level and square wave filtering frequency must be given together with the level of the sidebands.

### The pseudo-random noise method

The noise transfer method has been extensively used in telecommunications to indicate the so-called «loading noise» (i.e. intermodulation products) in carrier frequency and radio link equipment. The method consists of white noise input signal, of which a band of frequencies has been filtered off, Fig. 10b. The measurement is performed using a matched band-pass filter, Fig. 10c, and by measuring the amplitude of the noise intermodulation products falling into this frequency band. When the filter center frequencies are changed the whole frequency range of a system can be covered.

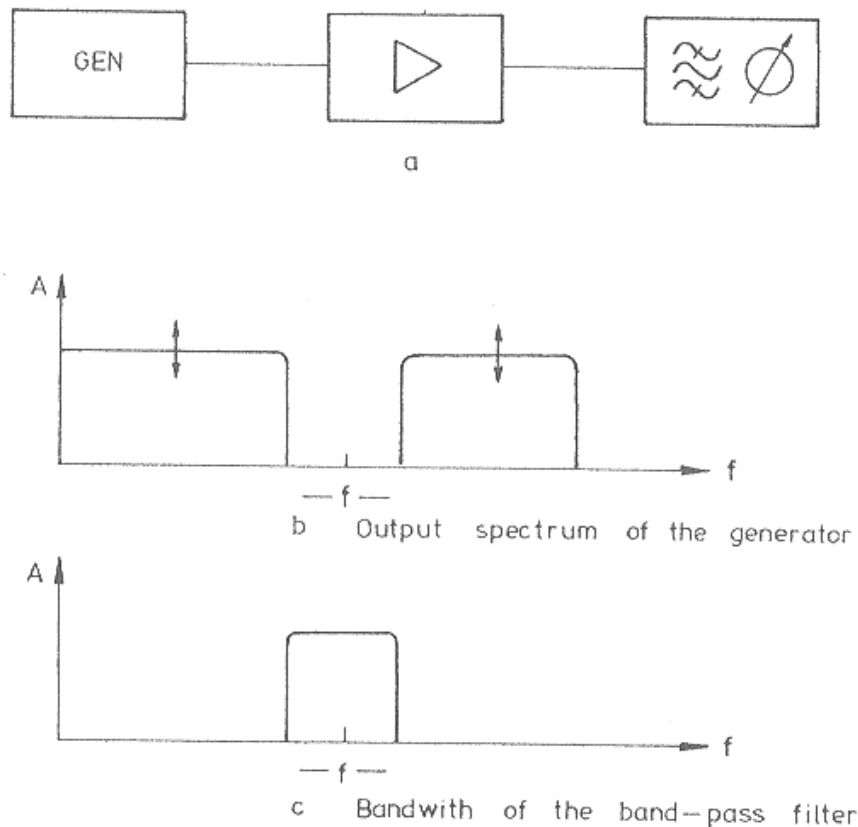


Fig. 10. Pseudo-random noise intermodulation method.

The theory of the method is readily understood and the results are well tabulated (see, for instance (6)). However, the application of this method to audio frequencies is difficult due to the expensive and bulky analogue filters.

This measurement can, however, be performed digitally by generating a band-limited pseudo-random noise input signal and by using digital filtering for the output signal. A proposed construction for the measuring instrument is shown in Fig. 11.

The instrument is controlled by a read-only memory *ROM* 1 and a micro-processor *CPU*, which governs two address counters *AC* 1 and *AC* 2. These generate phased alternative addresses for a read-only memory *ROM* 2. This memory contains the binary equivalent values of a  $(\sin x)/x$ -sequence, which has the character of a band-limited line spectrum. The frequency-offset phased two simultaneous  $(\sin x)/x$ -trains form the basic pseudo-random noise spectrum, which, with suitable choice of parameters, has a band of frequencies missing.

By changing the parameters, it is possible to sweep this frequency band, thus generating a noise-like measurement signal having a continuously swept band-reject characteristic. This digital signal is then converted into analogue form in an adder *A* and a digital-to-analogue converter *DAC*, and additionally filtered in a sweeping analogue band-reject filter *AR* 1.

The distorted signal from the output of the amplifier under test is band-pass filtered in a sweeping analogue filter *AF* 2, and subsequently converted into digital form in an analogue-to-digital converter *ADC*. The digital signal is fed into a comb-type digital filter, the results are processed in *CPU* and shown in display *D*.

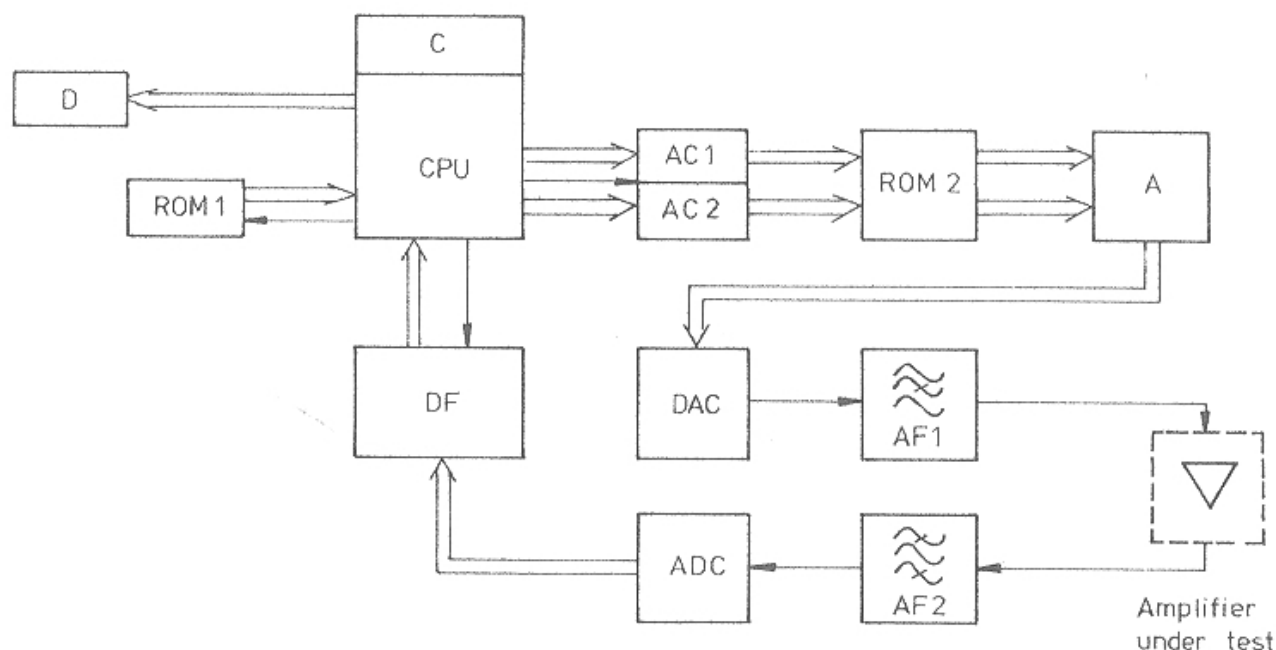


Fig. 11. A proposed construction of a pseudo-random noise intermodulation measurement instrument.

The physical realization of this instrument seems feasible with 12 bit *ADC* and *DAC*, and a 16 bit word length in the *CPU*. The merit of the design is that the instrument is capable, in principle, of distinguishing between *THD*, *IM* and *TIM* with suitable programming of the sequences and noise parameters. With the rapid decrease of the price of digital components, the total cost of the instrument should not be prohibitive in the near future.

## Conclusions

Three different measurement methods for the measurement of transient intermodulation distortion have been discussed. The overshoot clipping method is qualitatively quite sensitive, but necessitates penetration into the amplifier and is very tedious.

The square-wave intermodulation method is readily adaptable in certain existing distortion measurement instruments, and is both qualitatively and quantitatively sensitive and accurate.

The pseudo-random noise intermodulation method holds a promise for the automated distortion testing of amplifiers, but must still be considered to be in an embryo stage. It will, however, probably be a universal method, capable of detecting all distortion components, irrespective of their origin.

### References

1. OTALA, M., Transient distortion in transistorized audio power amplifiers. IEEE Transactions on Audio and Electroacoustics, AU-18(1970)3, p. 234–239.
2. OTALA, M. & LEINONEN, E., The theory of the transient intermodulation distortion. Monitor-Proc. IREE 37(1976)5, p. 53–59.
3. OTALA, M. & ENSOMAA, R., Transient intermodulation distortion in commercial audio amplifiers. Journal of the AES 22(1974)4, p. 244–246.
4. SCHROCK, C., Standard audio tests. Beaverton, Tektronix Inc., 1975, p. 17–18.
5. Test-noise signals for use in the measurement of non-linear distortion. London 1974. B.B.C. Research Department Report No. 640, p. 195–196.
6. FAGOT, J. & MAGNE, P., Frequency modulation theory. Application to microwave links. Oxford, Pergamon Press, 1961. 488 p.

## ELECTRICAL AND NUCLEAR TECHNOLOGY. Publications

1. Ekberg, Jan. On the properties of random pulse positioncode modulation: a system especially developed for the enciphering of speech signals. 1973. 62 p. + app. 9 p.
2. Reijonen, H., Kormano, M. & Reijonen, K., Comparison of X-ray and neutron radiography of pathological bone samples. 1973. 15 p.
3. Fahlenius, Aro. On the excitation of characteristic TiK, NbK and AuM x-rays by 0.7...2.5 MeV proton bombardment. 1973. 14 p.
4. Reijonen, H. & Jauho, P., On the determination of Pu<sup>239</sup> and Pu<sup>240</sup> from reactor fuel by neutron radiography with filtered neutron beams. 1973. 12 p.
5. Reijonen, Heikki. Neutron and gamma radiography with a research reactor. 1973. 11 p.
6. Kärkkäinen, Seppo. Physical mechanisms of partial discharges. 1974. 59 p. + app. 2 p.
7. Salo, Timo. Barriers model for the conduction mechanism in trigonal selenium crystals. 1973. 36 p.
8. Silvennoinen, P. & Tuominen, J., Curved low order angular elements in two-dimensional neutron transport problems. 1974. 15 p.
9. Krusius, Peter. The electronic structure of trigonal selenium. 1974. 33 p.
10. Saranummi, Niilo. On the elimination of some factors decreasing the accuracy of a resistivity transducer when sizing blood cells. 1975. 39 p. + app. 6 p.
11. von Boehm, Juhani. Applicability of the self-consistent orthogonalized-plane-wave method to the anisotropic semiconductors trigonal selenium and titanium disulphide. 1975. 28 p.
12. Mattila, L., Sairanen, R. & Stengard, J.-O., Estimation of the core-wide fuel rod damage during a LWR LOCA. 1975. 23 p.
13. Sinkkonen, J., Theory of anomalous Hall effect in europium chalcogenides. 1976. 48 p. + app. 30 p.
14. Kärkkäinen, Seppo. Internal partial discharges – pulse distributions, physical mechanisms and effects on insulations. 1976. 108 p. + 17 p.

Sale: Valtion painatuskeskus  
PL 516  
00101 Helsinki 10  
tel. 90-539011

ISBN 951-38-0395-3  
ISSN 0355-3396